

# Chemical Science

Accepted Manuscript



This is an *Accepted Manuscript*, which has been through the Royal Society of Chemistry peer review process and has been accepted for publication.

*Accepted Manuscripts* are published online shortly after acceptance, before technical editing, formatting and proof reading. Using this free service, authors can make their results available to the community, in citable form, before we publish the edited article. We will replace this *Accepted Manuscript* with the edited and formatted *Advance Article* as soon as it is available.

You can find more information about *Accepted Manuscripts* in the [Information for Authors](#).

Please note that technical editing may introduce minor changes to the text and/or graphics, which may alter content. The journal's standard [Terms & Conditions](#) and the [Ethical guidelines](#) still apply. In no event shall the Royal Society of Chemistry be held responsible for any errors or omissions in this *Accepted Manuscript* or any consequences arising from the use of any information it contains.

## ARTICLE

## Thymine Functionalised Porphyrins, Synthesis and Heteromolecular Surface-based Self-assembly.

Anna G. Slater,<sup>1†</sup> Ya Hu,<sup>2†</sup> Lixu Yang,<sup>1</sup> Stephen P. Argent,<sup>1</sup> William Lewis,<sup>1</sup> Matthew O. Blunt<sup>2\*</sup> and Neil R. Champness<sup>1\*</sup>

Cite this: DOI: 10.1039/x0xx00000x

Received 00th January 2012,  
Accepted 00th January 2012

DOI: 10.1039/x0xx00000x

www.rsc.org/

The synthesis and surface-based self-assembly of thymine-functionalised porphyrins is described. Reaction of 1-formylphenyl-3-benzoyl-thymine with suitable pyrrolic species leads to the formation of tetra-(phenylthymine)porphyrin (tetra-TP) or mono-thymine-tri-(3,5-di-*tert*-butylphenyl)porphyrin (mono-TP). Single crystal X-ray diffraction studies demonstrate the self-association of mono-TP in the solid state through thymine...thymine hydrogen-bonding interactions but in solution this interaction ( $K_d = 6.1 \pm 3.0 \text{ M}^{-1}$ ) is relatively weak in comparison to the heteromolecular interaction between mono-TP and 9-propyladenine ( $K = 91.8 \pm 20.5 \text{ M}^{-1}$ ). STM studies of the tetratopic hydrogen-bonding tecton, tetra-TP, deposited on an HOPG substrate reveal the formation of an almost perfectly square self-assembled lattice through thymine...thymine hydrogen-bonding. Co-deposition of tetra-TP with 9-propyladenine leads to the adoption of preferable thymine...adenine interactions leading to the formation of a heteromolecular tetra-TP...9-propyladenine hydrogen bonded array including both Watson-Crick thymine...adenine interactions and adenine...adenine hydrogen-bonding. The studies demonstrate a pathway for the self-assembly of tetratopic hydrogen-bonding tectons and the use of preferential heteromolecular thymine...adenine interactions for the disruption of the homomolecular tetra-TP array. Studies of the self-assembly of tetra-TP and 9-propyladenine demonstrate a strong dependence on overall concentration and molar ratio of components indicating the importance of kinetic effects in surface self-assembly processes.

### Introduction

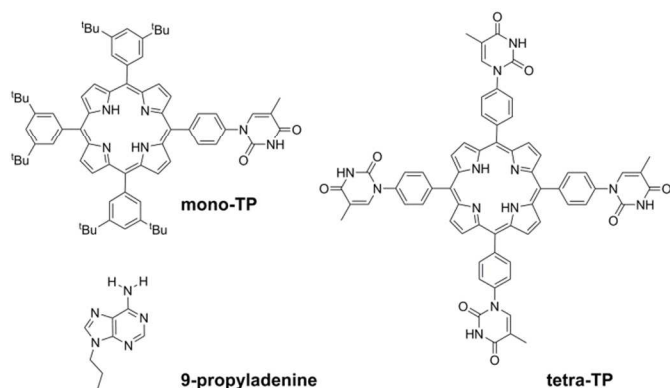
The study of self-assembled two-dimensional structures on surfaces has become an area of intense interest over recent years.<sup>1-5</sup> Particular focus has been applied to the use of intermolecular interactions in attempts to control the relative organisation of molecules and to create well-defined molecular arrangements. Intermolecular interactions that have been successfully used to prepare self-assembled structures include coordination bonds,<sup>6,7</sup> halogen bonds<sup>8,9</sup> and van der Waals interactions.<sup>10-12</sup> Hydrogen-bonds<sup>13-21</sup> have received extensive attention with a major focus being the exploitation of molecules bearing multiple carboxylic acids to form extended arrays.<sup>13-18</sup> It is also possible to prepare surface-based self-assembled structures from more than one molecular component<sup>22</sup> using the well-established concepts within supramolecular chemistry of the molecular tecton<sup>23,24</sup> and supramolecular synthon.<sup>25</sup> By using two or more tectons that are designed such that they incorporate hydrogen-bonding moieties that favour heteromolecular interactions multi-component arrays can be targeted.<sup>19-21</sup>

Perhaps the most widely known heteromolecular synthons are those formed between DNA nucleobases. Nucleobases have been extensively studied in the field of surface-based self-assembly with a particular focus on understanding their

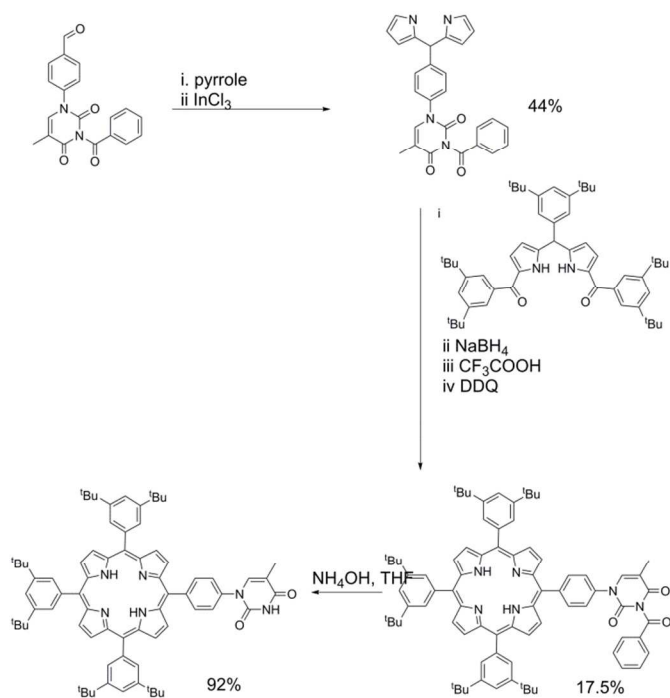
hydrogen-bonding behaviour. Two recent reviews cover advances in the area<sup>26,27</sup> and illustrate the complexity of such systems. Nucleobases have been studied using scanning tunnelling microscopy<sup>28-31</sup> including thymine (T)<sup>30</sup> and adenine (A),<sup>31</sup> of particular relevance to this study. Throughout these studies a variety of substrates have been used, including metallic surfaces and highly-ordered pyrolytic graphite (HOPG), as well as a variety of conditions, ultra-high vacuum and solid-liquid interfaces. A study of particular interest is that by Besenbacher *et al.* who describe studies that combine thymine and adenine.<sup>32</sup> As anticipated intermolecular hydrogen-bonding interactions are observed between the thymine and adenine generating A-T-A-T quartets that involve reverse Hoogsteen hydrogen-bonding. Examples of functionalized adenine and thymine molecules have been studied in attempts to influence the nature of the intermolecular hydrogen-bonding interactions. Notable examples, described by Bonifazi and co-workers,<sup>33,34</sup> report the synthesis of di-uracil rods and their subsequent self-assembly with molecules that present hydrogen-bonding motifs complementary to that of uracil (and thymine).

In this study we have synthesised thymine-functionalised porphyrin molecules, or tectons, (Scheme 1) that present the imide hydrogen bonding moiety of thymine in such a manner to encourage divergent assembly with either other molecules of

the same type or with a simple propyl-functionalised adenine species, 9-propyl-9H-purine-6-ylamine (9-propyladenine). Porphyrins represent useful scaffolds for the basis of hydrogen-bonding tectons as functionalization of each meso-position leads to a tetratopic tecton. The vast majority of tectons previously investigated in surface self-assembled networks<sup>1-5</sup> are either rod-like ditopic tectons<sup>6,13,19-21</sup> or tritopic<sup>7,12,14,19-21</sup> tectons. Although tetratopic hydrogen-bonding tectons are known, notably with carboxylic acid groups,<sup>15-18</sup> systems with more specific hydrogen-bonding moieties for heteromolecular arrays have not been studied previously for surface self-assembly. Porphyrins present a highly attractive target for the basis of tetratopic tectons due to their fourfold symmetry and have been used for the assembly of a variety of surface-based self-assembled structures<sup>35</sup> including covalently-coupled arrays<sup>36</sup> and, notably with carboxylic acid hydrogen-bonding moieties through the use of 5,10,15,20-tetrakis-(4-carboxylphenyl)-porphyrin.<sup>37</sup>



Scheme 1. Molecules used in this study.



Scheme 2. Synthetic route used for the preparation of mono-TP.

Two target porphyrin molecules were identified: tetra-(phenylthymine)porphyrin (tetra-TP) for surface-based self-assembly studies and mono-thymine-tri-(3,5-di-*tert*-butylphenyl)porphyrin (mono-TP) as a model compound to probe the nature of intermolecular interactions in the solution phase. The basic design encompassed functionalisation of the porphyrin core with phenylthymine groups and the remaining meso positions, in the case of mono-TP, bearing 3,5-di-*tert*-butylphenyl moieties. The *tert*-butyl functionalised appendages were chosen due to their ability to enhance porphyrin solubility, inhibiting  $\pi$ - $\pi$  interactions, and allowing more facile solution-based studies. The synthesis of a porphyrin functionalised with uracil in the meso-position, 10,15,20-tetrakis(1-butyl-6-uracyl)porphyrin, has been reported previously<sup>38</sup> and was found to form nanofibre structures. The design of 10,15,20-tetrakis(1-butyl-6-uracyl)porphyrin is not appropriate for surface self-assembly studies due to the orthogonal arrangement of the uracil moiety with respect to the porphyrin core. Thus we adopted a design that positioned a phenyl group between the porphyrin plane and the thymine group so that both porphyrin and thymine could be co-planar and parallel to the surface that the molecules were to be deposited upon. Our studies demonstrate that it is not only possible to prepare homomolecular hydrogen-bonded arrays with tetra-TP but heteromolecular arrays can be generated by combination of suitable tectons, in our case tetra-TP and 9-propyladenine.

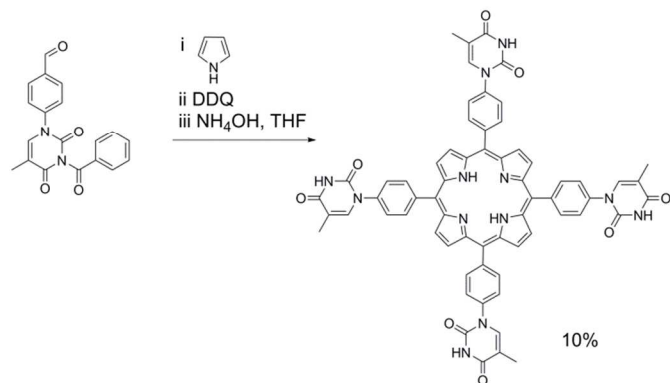
## Results and Discussion

### Synthesis and structural studies

Porphyrin molecules were prepared functionalised in the meso-positions by phenyl-thymine moieties. Our approach required the synthesis of 1-formylphenyl-3-benzoyl-thymine from 4-formylphenylboronic acid and 3-benzoylthymine<sup>39</sup> using a  $\text{Cu}(\text{OAc})_2$ -mediated Chan-Lam-Evans-modified Ullmann condensation reaction to facilitate the cross-coupling process.<sup>40</sup> Reaction of 1-formylphenyl-3-benzoyl-thymine with a large excess of pyrrole in the presence of  $\text{InCl}_3$  affords the desired dipyrromethane which can be subsequently used in porphyrin synthesis.

In the case of mono-TP the benzoyl-thymine functionalised dipyrromethane was reacted with a suitable *tert*-butyl functionalised carbinol species, using Lindsay's approach,<sup>41</sup> in the presence of trifluoroacetic acid (TFA) with subsequent oxidation using 2,3-dichloro-5,6-dicyano-1,4-benzoquinone (DDQ), see Scheme 1 (mono-TP). Subsequent deprotection of the benzoyl-protected thymine was achieved in good yield using  $\text{NH}_4\text{OH}$  as the deprotecting agent.<sup>42</sup> The synthesis of the tetra-TP was more straightforward (Scheme 3) following direct reaction of 1-formylphenyl-3-benzoyl-thymine with a large excess of pyrrole using TFA to initiate the reaction. Oxidation with DDQ gave the target molecule in 11% yield and deprotection, again using  $\text{NH}_4\text{OH}$ ,<sup>42</sup> afforded tetra-TP in 91% yield.

The products were characterised by conventional techniques and in the case on mono-TP and its benzoyl-protected precursor by single crystal X-ray diffraction. For both of these compounds slow diffusion of MeOH into a solution of the compound, either  $\text{CH}_2\text{Cl}_2$  (mono-TP) or  $\text{CDCl}_3$  (benzoyl-mono-TP), led to growth of single crystals of suitable quality for X-ray diffraction studies. In both cases the X-ray structure confirms the identity of the product and the relative arrangement of the thymine moiety with respect to the porphyrin ring (Figure 1).



**Scheme 3.** Synthetic route used for the preparation of tetra-TP.

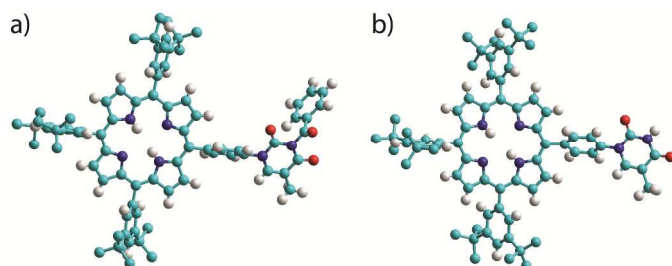


**Figure 1.** Single crystal X-ray structures of (a) benzoyl-mono-TP and (b) mono-TP. Note the relative orientation of the thymine moiety with respect to the porphyrin plane. Hydrogen atoms of the tert-butyl groups are omitted for clarity. Atoms are colored as follows C – light blue; N – dark blue; H – white; O – red.

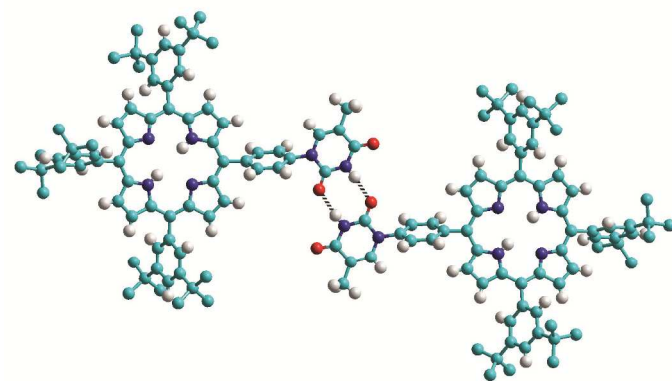


**Figure 2.** View of the single crystal X-ray structure of mono-TP illustrating the formation of the inter-thymine  $R_2^2(8)$  double hydrogen-bonding interaction (represented with the two dotted lines) observed in the solid state. Hydrogen atoms of the tert-butyl groups are omitted for clarity. Atoms are colored as follows C – light blue; N – dark blue; H – white; O – red.

The structure of the mono-TP reveals valuable information about the nature of the intermolecular interactions anticipated for thymine-substituted porphyrin species (Figure 2). The most pertinent feature is the formation of an  $R_2^2(8)$  double hydrogen-bonding interaction<sup>43</sup> between thymine moieties on adjacent molecules. Each N-H...O hydrogen bond within the inter-thymine  $R_2^2(8)$  synthon is crystallographically equivalent

[N...O = 2.818(3); H...O = 1.94; < N-H...O = 172.0] and falls within the typical range expected for such a hydrogen bond.<sup>44</sup> Adjacent molecules pack such that  $\pi$ - $\pi$  interactions are observed between the thymine moiety of one molecule and a pyrrole of an adjacent molecule (centroid...centroid separation of 3.50Å). As anticipated in both structures, benzoyl-mono-TP and mono-TP, the phenyl ring that links the porphyrin moiety with the thymine group adopts an orientation that approaches orthogonality (71.02°:benzoyl-mono-TP; 64.01°:mono-TP) and the thymine approaches co-planarity with the porphyrin core in both instances (17.21°:benzoyl-mono-TP; 13.37°:mono-TP).

In order to assess the strength of interaction between porphyrin-appended thymine moieties and a simple propyl-functionalised adenine species, 9-propyl-9H-purine-6-ylamine (9-propyladenine), a series of binding studies were undertaken using solutions of mono-TP in CDCl<sub>3</sub> solution, see SI for details,<sup>45</sup> (tetra-TP was found to be have insufficient solubility in suitable solvents to allow binding studies). The possibility of self-association needs to be considered, particularly considering the observed thymine...thymine interactions in the single crystal structure of mono-TP. Thus self-association binding constants were measured for mono-TP ( $K_d = 6.1 \pm 3.0 \text{ M}^{-1}$ ) and 9-propyladenine ( $K_d = 2.8 \pm 1.7 \text{ M}^{-1}$ ) and found to be small in both instances. In contrast the binding constant for the interaction between mono-TP and 9-propyladenine was found to be  $K = 91.8 \pm 20.5 \text{ M}^{-1}$  indicating a favourable hetero-intermolecular interaction between the two species as anticipated. The NMR studies also indicate both Hoogsteen<sup>46</sup> and Watson-Crick<sup>47</sup> binding modes between the thymine and adenine moieties with corresponding shifts in the C8-H and C2-H proton signals respectively (Figure 3).

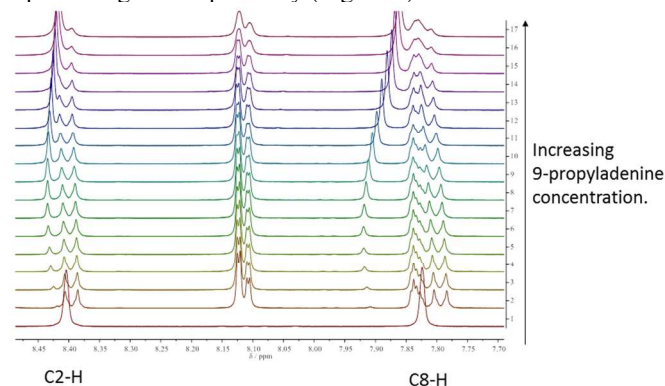


**Figure 3.** <sup>1</sup>H NMR spectrum illustrating shifts in the C8-H and C2-H proton signals during titration of mono-TP with 9-propyladenine. Spectrum 1 corresponds to pure 9-propyladenine and spectra 2-17 are recorded with constant mono-TP concentration and increasing 9-propyladenine concentration.

### Surface Self-Assembly Studies

The surface self-assembly of tetra-TP and 9-propyladenine was investigated at liquid-solid interfaces between highly oriented pyrolytic graphite (HOPG) and an organic solvent layer using scanning tunnelling microscopy (STM). All attempts to adsorb mono-TP onto HOPG were unsuccessful which we attribute to weaker adsorption of this molecule on this surface under the conditions used, in part due to the enhanced solubility of this molecule in comparison to tetra-TP and the smaller number of potential intermolecular hydrogen-bonding interactions. Mixtures of tetrahydrofuran (THF) and 1,2,4-trichlorobenzene (TCB) with a 1:9 volume ratio respectively were used as

solvents for the tetra-TP and 9-propyladenine. Solutions in the concentration range  $5 \times 10^{-6}$  to  $5 \times 10^{-5}$  M for tetra-TP and  $8 \times 10^{-6}$  to  $1 \times 10^{-3}$  M for the 9-propyladenine were employed. Even at these low concentrations the tetra-TP solutions were saturated with some visible undissolved material. It was found that saturated solutions were required in order to form self-assembled surface structures. A small quantity of saturated solution was deposited on to a preheated HOPG substrate held at  $60^\circ\text{C}$ . After 5 minutes held at this temperature the substrate was allowed to cool naturally before STM imaging.

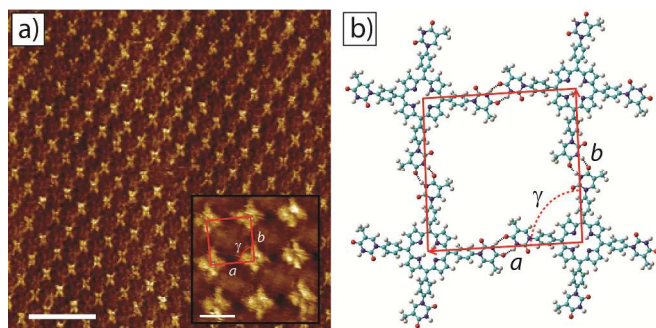


**Figure 4.** 2D self-assembled network of tetra-TP at the TCB-HOPG liquid-solid interface. a) Large scale STM image of the tetra-T-porphyrin ( $2.82 \times 10^{-5}$  M) network at the TCB-HOPG liquid-solid interface. The insert shows a high resolution, drift corrected STM image of the network with an individual 2D unit cell marked in white: unit cell parameters  $a = 25.9 \pm 0.5$  Å;  $b = 25.2 \pm 0.6$  Å; and  $\gamma = 91 \pm 1^\circ$ . STM imaging parameters:  $V_s = -0.5\text{V}$ ;  $I_t = 15\text{pA}$ . Scale bar = 20nm (insert = 2nm). b) Molecular model of the tetra-T-porphyrin network from MM simulations. Unit cell parameters  $a = 26.0$  Å;  $b = 25.9$  Å; and  $\gamma = 90^\circ$ .

STM images of tetra-TP self-assembled structures clearly display the cruciform shape and symmetry of the tetra-TP molecules suggesting they adsorb in a planar fashion on the HOPG substrate (Figure 4a). The self-assembled structure displays large domains,  $> 100$  nm, of a hydrogen bond stabilised network with a P2 plane symmetry group. Analysis of drift corrected STM images (Figure 4a insert) provide 2D unit cell dimensions for this structure of  $a = (25.9 \pm 0.5)$  Å;  $b = (25.2 \pm 0.6)$  Å and  $\gamma = (90 \pm 2)^\circ$  and angles between the unit cell vectors and underlying HOPG symmetry axes of  $\alpha = (6 \pm 3)^\circ$ ; and  $\beta = (25 \pm 3)^\circ$ . For details of the drift correction process applied to the STM images see the SI.

Figure 4b shows a structural model derived from molecular mechanics (MM) simulations for the tetra-TP network. This molecular structure is stabilised by thymine-thymine hydrogen bond dimers formed between adjacent tetra-TP molecules, in a similar fashion to the bonding arrangement observed in the single crystal structure of mono-TP. The inter-thymine hydrogen-bonding arrangement is also similar to that observed for thymine adsorbed at the liquid-solid interface between 1-octanol and HOPG.<sup>32</sup> Additionally tetrakis(4-carboxy-phenyl)-porphyrin molecules adopt a similar hydrogen bond stabilised structure on an Au(111) surface<sup>37c</sup> where the network is stabilised via carboxylic acid hydrogen bond dimers. The MM simulations were carried out with the molecules placed above a single fixed layer of graphene; further details of the simulations are available in the SI. Unit cell dimensions and measured from geometry optimised structures produced values of  $a = 26.0$  Å;  $b = 25.9$  Å and  $\gamma = 91^\circ$  and angles between the unit cell vectors and underlying graphite symmetry axes of  $\alpha = 4.7^\circ$ ; and  $\beta = 24.3^\circ$ , in good agreement with the experimentally determined values.

The asymmetric nature of the thymine groups decorating the tetra-TP molecules indicates that the molecules have the potential to adopt a chiral arrangement when adsorbed onto a surface.<sup>48</sup> Numerous previous studies have shown that prochiral molecules tend to assemble into homochiral domains on surfaces containing molecules of only a single handedness.<sup>49</sup> The almost perfectly square 2D unit cell observed for the tetra-TP structure suggests that all of the thymine groups within an individual tetra-TP molecule display the same orientation with respect to the porphyrin core, and that individual domains contain only molecules of a single handedness. The overall surface structure of tetra-TP remains globally achiral by forming an equal area of mirror domains containing either right, or left-handed molecules. STM images showing the mirror image tetra-TP domain to that observed in Figure 4 are shown in the SI. There is no significant barrier to rotation of the thymine groups prior to surface adsorption and although we see no evidence of porphyrin molecules with mixed thymine orientations we cannot rule out the possibility of such orientations existing in small localised regions.

The surface self-assembly of mixtures of tetra-TP and 9-propyladenine on HOPG produced a molecular network with a combination of disordered regions interspersed with small domains of an ordered co-crystal structure containing both tetra-TP and 9-propyladenine. Figure 5a shows a large scale STM image displaying both the disordered structure (top right hand corner) and the ordered co-crystal (top left hand corner). Analysis of high resolution drift corrected STM images for the tetra-TP / 9-propyladenine co-crystal (Figure 5a insert) produce unit cell dimensions of  $a = (25.4 \pm 0.7)$  Å;  $b = (22.2 \pm 0.9)$  Å and  $\gamma = (83.0 \pm 2.0)^\circ$  and angles between the unit cell vectors and underlying HOPG symmetry axes of  $\alpha = (4.4 \pm 1.2)^\circ$ ; and  $\beta = (26.9 \pm 2.1)^\circ$ .

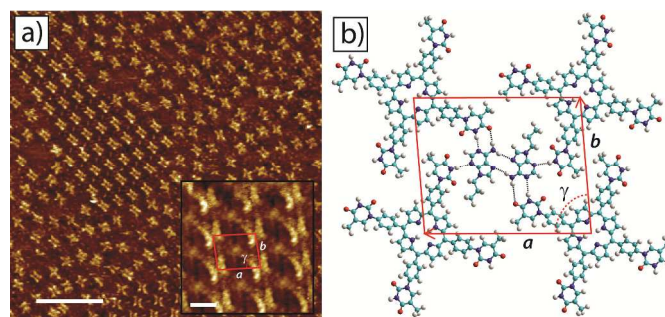


**Figure 5.** 2D self-assembled network of tetra-TP and 9-propyladenine at the TCB-HOPG liquid-solid interface. a) Large scale STM image of the tetra-TP ( $2.82 \times 10^{-5}$  M) and 9-propyladenine ( $4.52 \times 10^{-4}$  M) network at the TCB-HOPG liquid-solid interface. The insert shows a high resolution, drift corrected STM image of the network with an individual 2D unit cell marked in red: unit cell parameters from STM images  $a = 25.4 \pm 0.7$  Å;  $b = 22.2 \pm 0.9$  Å; and  $\gamma = 83 \pm 2^\circ$ . STM imaging parameters:  $V_s = -0.5\text{V}$ ;  $I_t = 15\text{pA}$ . Scale bar = 200 Å (insert = 16 Å). b) Molecular model of the tetra-T-porphyrin network from MM simulations. Unit cell parameters from MM simulations  $a = 26.0$  Å;  $b = 21.5$  Å; and  $\gamma = 85.7^\circ$ .

Using the same method as adopted for the tetra-TP network MM simulations were performed to produce a molecular model for the tetra-TP and 9-propyladenine co-crystal network (Figure 5b). This structure consists of a pair of 9-propyladenine molecules surrounded by 4 tetra-TP molecules. The 9-propyladenine molecules are linked to each other in a dimeric hydrogen bonded arrangement and each 9-propyladenine is further linked to the surrounding tetra-TP molecules by three

hydrogen bonds. The dimeric arrangement of the two 9-propyladenine molecules is the same as that calculated to be the most stable arrangement and previously observed for unfunctionalised adenine adsorbed on HOPG.<sup>32</sup> Two of the hydrogen bonds linking the 9-propyladenine to one of the neighbouring tetra-TP molecules adopt a Watson-Crick<sup>47</sup> binding mode. The remaining available hydrogen-bonded site on 9-propyladenine, the N3 position, adopts a conventional N-H...N hydrogen bond to a further tetra-TP molecule. Unit cell dimensions measured from geometry optimised MM simulations gave values of  $a = 26.0 \text{ \AA}$ ;  $b = 21.5 \text{ \AA}$ ; and  $\gamma = 85.7^\circ$ . The angles between the unit cell vectors and underlying graphite symmetry axes were  $\alpha = 4.7^\circ$ ; and  $\beta = 30.0^\circ$ , in good agreement with the experimentally determined values. Similarly to the tetra-TP network, the tetra-TP and 9-propyladenine co-crystal also displays the formation of homochiral domains in which the thymine groups of the chiral tetra-TP molecule all adopt the same orientation with respect to the porphyrin core. An STM image displaying two mirror image domains of the tetra-TP and 9-propyladenine co-crystal is provided in the SI.

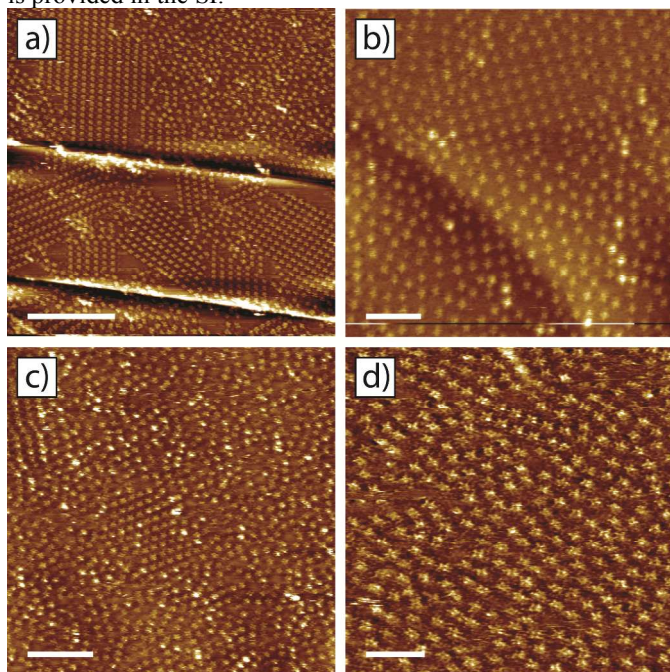


**Figure 6** Influence of the concentration and molar ratio of components on the morphology of the tetra-TP / 9-propyladenine network. a) Tetra-TP ( $1.41 \times 10^{-5} \text{ M}$ ) and 9-propyladenine ( $2.26 \times 10^{-4} \text{ M}$ ) mixture: molar ratio 1:16. b) Tetra-TP ( $3.03 \times 10^{-5} \text{ M}$ ) and 9-propyladenine ( $8.07 \times 10^{-6} \text{ M}$ ) mixture: molar ratio 4:1. c) Tetra-TP ( $1.77 \times 10^{-5} \text{ M}$ ) and 9-propyladenine ( $1.13 \times 10^{-3} \text{ M}$ ) mixture: molar ratio 1:64. d) Tetra-T-porphyrin ( $5.04 \times 10^{-6} \text{ M}$ ) and propyl adenine ( $1.93 \times 10^{-3} \text{ M}$ ) mixture: molar ratio 1:383. STM imaging parameters:  $V_s = -0.5 \text{ V}$ ;  $I_t = 15 \text{ pA}$ . Scale bars: a) 40 nm; b) 10 nm; c) 20 nm; d) 10 nm.

The domain size for the tetra-TP and 9-propyladenine co-crystal and the prevalence of the disordered structure are linked to both the concentration and ratio of the individual components. Figure 6a-d shows four example STM images of structures produced using different concentrations and molar ratios of tetra-TP and 9-propyladenine. Figure 6a has the same molar ratio of tetra-TP to 9-propyladenine, 1:16, as Figure 5a but half the overall molar concentration. The domain size for the tetra-TP and 9-propyladenine co-crystal has increased at the expense of the disordered arrangement.

Figure 6b has the same molar concentration of tetra-TP as Figure 5a but a greatly reduced concentration of 9-propyladenine so that in this case the molar ratio of tetra-TP to 9-propyladenine is 4:1. In this case the tetra-TP and 9-propyladenine co-crystal structure is not present; instead we observe the disordered network interspersed with domains of the tetra-TP mono-component network. As the amount of 9-propyladenine in the mixture is increased domains of the tetra-TP and 9-propyladenine co-crystal reduce in size until we are left with primarily the disordered structure. This effect can be seen in Figure 6c and Figure 6d which show example STM images of mixtures with molar ratios of tetra-TP to 9-propyladenine of 1:64 and 1:383 respectively. The delicate dependence of the co-crystal structure on the concentration and molar ratio of the components suggests that kinetic effects play a critical role in the self-assembly of tetra-TP and 9-propyladenine.

## Conclusions

We have demonstrated a successful strategy for employing tetratopic tectons in the preparation of surface-based self-assembled arrays. Inter-thymine hydrogen bonds successfully lead to the formation of square-grid lattices upon deposition of tetra-TP onto an HOPG substrate. The preferential formation of heteromolecular hydrogen-bonds exhibited by thymine and adenine decorated tectons, validated in solution by NMR studies, can be exploited to disrupt the homomolecular tetra-TP array and leads to the formation of a co-crystal between tetra-TP and 9-propyladenine. Studies of the self-assembly of tetra-TP and 9-propyladenine demonstrate a strong dependence on overall concentration and molar ratio of components. Lower overall concentrations lead to a greater proportion of ordered domains and the degree of order in the resulting structures is highly dependent on the molar ratio of tetra-TP:9-propyladenine. These studies indicate the importance of kinetic effects in surface self-assembly processes.

The system reported herein illustrates a successful strategy that has wide implications for the design of new tectons to be used in the formation of heteromolecular arrays. We demonstrate that the exploitation of the familiar recognition pathways of DNA bases can be incorporated into complex molecules and used to generate heteromolecular arrays. This approach has far-reaching implications for molecule/tecton design for preparing specific hydrogen-bonded arrays on surfaces and strongly indicates the possibility of preparing complex multicomponent arrays using a self-assembly stratagem.

## Experimental

Details of the synthetic procedures employed are described in the SI. The following intermediate species were synthesised following literature methods: 3,5-di-*tert*-butylbenzoic acid,<sup>50</sup> 3,5-di-*tert*-butylbenzaldehyde,<sup>51</sup> 3,5-di-*tert*-butylphenyl-dipyromethane,<sup>52</sup> 3-benzoylthymine<sup>39</sup> and 9-propyladenine.<sup>53</sup> CCDC-1034260 (mono-TP) and CCDC-1034261 (benzoyl-mono-TP) contain the supplementary crystallographic data for this paper. These data can be obtained free of charge from the Cambridge Crystallographic Data Centre via [www.ccdc.cam.ac.uk/data\\_request/cif](http://www.ccdc.cam.ac.uk/data_request/cif). Further details of the single crystal structure refinements are given in SI but details of the final refinement parameters are as follows for the structures of and benzoyl-mono-TP.

*Crystal Data for mono-TP*:  $C_{74}H_{86}N_6O_3$  ( $M = 1107.48$ ): triclinic, space group P-1 (no. 2),  $a = 9.8270(6) \text{ \AA}$ ,  $b = 16.9659(8) \text{ \AA}$ ,  $c =$

21.6298(13) Å,  $\alpha = 69.273(5)^\circ$ ,  $\beta = 81.505(5)^\circ$ ,  $\gamma = 87.976(5)^\circ$ ,  $V = 3335.2(4) \text{ \AA}^3$ ,  $Z = 2$ ,  $T = 120(2) \text{ K}$ ,  $\mu(\text{Synchrotron}) = 0.063 \text{ mm}^{-1}$ ,  $D_{\text{calc}} = 1.103 \text{ g/mm}^3$ , 31197 reflections measured, 11500 unique ( $R_{\text{int}} = 0.0549$ ) which were used in all calculations. The final  $R_1$  was 0.0756 ( $I > 2\sigma(I)$ ) and  $wR_2$  was 0.2097 (all data).

*Crystal Data for Mono-phenyl(benzoylthymine)-tri-(3,5-di-tert-butylphenyl)porphyrin.6 CHCl<sub>3</sub>*;  $\text{C}_{86}\text{H}_{92}\text{Cl}_{18}\text{N}_6\text{O}_3$  ( $M = 1895.75$ ): triclinic, space group P-1 (no. 2),  $a = 15.4721(5) \text{ \AA}$ ,  $b = 16.3717(5) \text{ \AA}$ ,  $c = 19.0278(6) \text{ \AA}$ ,  $\alpha = 92.068(2)^\circ$ ,  $\beta = 110.731(3)^\circ$ ,  $\gamma = 99.280(3)^\circ$ ,  $V = 4426.0(3) \text{ \AA}^3$ ,  $Z = 2$ ,  $T = 120(2) \text{ K}$ ,  $\mu(\text{Cu-K}\alpha) = 0.063 \text{ mm}^{-1}$ ,  $D_{\text{calc}} = 1.422 \text{ g/mm}^3$ , 52160 reflections measured, 15638 unique ( $R_{\text{int}} = 0.079$ ) which were used in all calculations. The final  $R_1$  was 0.1220 ( $I > 2\sigma(I)$ ) and  $wR_2$  was 0.3846 (all data).

Details of the STM experiments, image analysis and MM simulations can be found in the SI.

## Acknowledgements

We would like to gratefully acknowledge the support of Engineering and Physical Sciences Research Council (EP/H010432/1). YH gratefully acknowledges receipt of a UCL Overseas Research Scholarship (UCL-ORS). NRC gratefully acknowledges receipt of a Royal Society Wolfson Merit Award. MOB gratefully acknowledges the Marie Skłodowska-Curie actions research fellowship programme for the award of a Career Integration Grant (618777-PHOTOSURF).

## Notes and references

<sup>a</sup> School of Chemistry, University of Nottingham, University Park, Nottingham, NG7 2RD UK Address here.

<sup>b</sup> The Department of Chemistry, University College London (UCL), London, WC1H 0AJ, UK

† A.G. Slater and Y. Hu contributed equally to this work.

E-mail: [Neil.Champness@nottingham.ac.uk](mailto:Neil.Champness@nottingham.ac.uk); [m.blunt@ucl.ac.uk](mailto:m.blunt@ucl.ac.uk)

† Footnotes should appear here. These might include comments relevant to but not central to the matter under discussion, limited experimental and spectral data, and crystallographic data.

Electronic Supplementary Information (ESI) available: Additional experimental details including: full synthetic methods and characterization; full details of single crystal X-ray structure refinement and CIFs; binding measurements; STM experiments; and MM simulations. See DOI: 10.1039/b000000x/

## References

- A.G. Slater (née Phillips), P.H. Beton and N.R. Champness, *Chem. Sci.*, 2011, **2**, 1440-1448.
- J.A.A.W. Elemans, S. Lei and S. De Feyter, *Angew. Chem. Int. Ed.*, 2009, **48**, 7298-7332.
- F. Cicoira, C. Santato and F. Rosei, *Top. Curr. Chem.*, 2008, **285**, 203-267.
- L. Bartels, *Nature Chem.*, 2010, **2**, 87-95.
- J.V. Barth, G. Costantini and K. Kern, *Nature*, 2005, **437**, 671-679.
- S. Stepanow, M. Lingenfelder, A. Dmitriev, H. Spillmann, E. Delvigne, N. Lin, X.B. Deng, C.Z. Cai, J.V. Barth and K. Kern, *Nat. Mater.*, 2004, **3**, 229-233.
- S. Vijayaraghavan, D. Ecija, W. Auwaerter, S. Joshi, K. Seufert, M. Drach, D. Nieckarz, P. Szabelski, C. Aurisicchio, D. Bonifazi and J.V. Barth, *Chem. Eur. J.*, 2013, **19**, 14143-14150.
- J. K. Yoon, W.-j. Son, K.-H. Chung, H. Kim, S. Han and S.-J. Kahng, *J. Phys. Chem. C*, 2011, **115**, 2297-2301.
- R. Gutzler, C. Fu, A. Dadvand, Y. Hua, J.M. MacLeod, F. Rosei and D.F. Perepichka, *Nanoscale*, 2012, **4**, 5965-5971.
- M. Böhrringer, K. Morgenstern, W.-D. Schneider and R. Berndt *Angew. Chem. Int. Ed.*, 1999, **38**, 821-823.
- T. Yokoyama, S. Yokoyama, T. Kamikado, Y. Okuno and S. Mashiko, *Nature*, 2001, **413**, 619-621.
- M.O. Blunt, J. Adisoejoso, K. Tahara, K. Katayama, M. van der Auweraer, Y. Tobe and S. De Feyter, *J. Am. Chem. Soc.*, 2013, **135**, 12068-12075.
- J.V. Barth, J. Weckesser, C. Cai, P. Günter, L. Bürgi, O. Jeandupeux and K. Kern, *Angew. Chem. Int. Ed.*, 2000, **39**, 1230-1234.
- S. Griessl, M. Lackinger, M. Edelwirth, M. Hietschold and W.M. Heckl, *Single Mol.*, 2002, **3**, 25-31.
- H. Zhou, H. Dang, J.-H. Yi, A. Nanci, A. Rochefort and J.D. Wuest, *J. Am. Chem. Soc.*, 2007, **129**, 13774-13775.
- M. Li, K. Deng, S.-B. Lei, Y.-L. Yang, T.-S. Wang, Y.-T. Shen, C. Wang, Q.-D. Zeng and C. Wang, *Angew. Chem., Int. Ed.*, 2008, **47**, 6717-6721.
- M.O. Blunt, J. Russell, M.C. Giménez-López, J.P. Garrahan, X. Lin, M. Schröder, N.R. Champness and P.H. Beton, *Science*, 2008, **322**, 1077
- M.O. Blunt, J.C. Russell, M.C. Gimenez-Lopez, N. Taleb, X. Lin, M. Schröder, N.R. Champness and P.H. Beton, *Nat. Chem.*, 2011, **3**, 74-78.
- J.A. Theobald, N.S. Oxtoby, M.A. Phillips, N.R. Champness and P.H. Beton, *Nature*, 2003, **424**, 1029-1031.
- M.T. Räisänen, A.G. Slater (née Phillips), N.R. Champness and M. Buck, *Chem. Sci.*, 2012, **3**, 84-92.
- R. Madueno, M.T. Räisänen, C. Silien and M. Buck, *Nature*, 2008, **454**, 618-621.
- A.G. Slater, L.M.A. Perdigo, P.H. Beton and N.R. Champness, *Acc. Chem. Res.*, 2014, *in press*, DOI: 10.1021/ar5001378.
- M.W. Hosseini, *Acc. Chem. Res.*, 2005, **38**, 313-323.
- M. Simard, D. Su and J.D. Wuest, *J. Am. Chem. Soc.*, 1991, **113**, 4696-4698.
- G.R. Desiraju, *Angew. Chem. Int. Ed.*, 1995, **34**, 2311-2327.
- L. Liu, D. Xia, L.H. Klausen and M. Dong, *Int. J. Mol. Sci.* 2014, **15**, 1901-1914
- L. Liu, F. Besenbacher, M. Dong, *Nucleic Acid Nanotechnology*, Ed.: J. Kjems, E. Ferapontova, K.V. Gothelf, Book Series: Nucleic Acids and Molecular Biology, 2014, **29**, 3-21.
- For studies of guanine see: (a) R. Otero, M. Schock, L.M. Molina, E. Laegsgaard, I. Stensgaard, B. Hammer and F. Besenbacher, *Angew. Chem. Int. Ed.*, 2005, **44**, 2270-2275. (b) H. Kong, Q. Sun, L. Wang, Q. Tan, C. Zhang, K. Sheng and W. Xu, *ACS Nano*, 2014, **8**, 1804-1808. (c) A. Ciesielski, S. Lena, S. Masiero, G. Piero Spada and P. Samori, *Angew. Chem. Int. Ed.*, 2010, **49**, 1963-1966. (d) A. Ciesielski, R. Perone, S. Pieraccini, G. Piero Spada and P. Samori, *Chem. Commun.*, 2010, **46**, 4493-4495.
- For studies of cytosine see: (a) R. Otero, M. Lukas, R.E.A. Kelly, W. Xu, E. Lægsgaard, I. Stensgaard, L.N. Kantorovich and F.

- Besenbacher, *Science*, 2008, **319**, 312-315. (b) D.J. Frankel, Q. Chen and N.V. Richardson, *J. Chem. Phys.*, 2006, **124**, 204704. (c) H. Kong, L. Wang, Q. Tan, C. Zhang, Q. Sun and W. Xu, *Chem. Commun.*, 2014, **50**, 3242-3244.
30. For studies of thymine see: (a) B. Roelfs, E. Bunge, C. Schröter, T. Solomun, H. Meyer, R.J. Nichols and H. Baumgärtel, *J. Phys. Chem. B* 1997, **101**, 754-765. (b) A. Chatterjee, L. Zhang and K.T. Leung, *J. Phys. Chem. C*, 2013, **117**, 14677-14683.
31. For studies of adenine see: (a) A. Maleki, S. Alavi and B. Najafi, *J. Phys. Chem. C*, 2011, **115**, 22484-22494. (b) Z. Mu, O. Rubner, M. Bamler, T. Blöker, G. Kehr, G. Erker, A. Heuer, H. Fuchs and L. Chi, *Langmuir*, 2013, **29**, 10737-10743. (c) S.J. Sowerby, M. Edelwirth and W.M. Heckl, *J. Phys. Chem. B*, 1998, **102**, 5914-5922. (d) Q. Tan, C. Zhang, N. Wang, X. Zhu, Q. Sun, M.F. Jacobsen, K.V. Gothelf, F. Besenbacher, A. Hu and W. Xu, *Chem. Commun.*, 2014, **50**, 356-358. (e) A. Chatterjee, L. Zhang and K.T. Leung, *Langmuir*, 2013, **29**, 9369-9377. (f) L.M.A. Perdigão, P.A. Staniec, N.R. Champness, R.E.A. Kelly, L.N. Kantorovich and P.H. Beton, *Phys. Rev. B*, 2006, **73**, 195423. (g) Q. Chen, D.J. Frankel and N.V. Richardson, *Langmuir*, 2003, **18**, 3219-3225. (h) Q. Chen and N.V. Richardson, *Nat. Mater.*, 2003, **2**, 324-328.
32. W. Mamdouh, M. Dong, S. Xu, E. Rauls and F. Besenbacher, *J. Am. Chem. Soc.*, 2006, **128**, 13305-13311.
33. C.-A. Palma, J. Bjork, M. Bonini, M.S. Dyer, A. Llanes-Pallas, D. Bonifazi, M. Persson and P. Samori, *J. Am. Chem. Soc.*, 2009, **131**, 13062-13071.
34. A. Llanes-Pallas, M. Matena, T. Jung, M. Prato, M. Stöhr, D. Bonifazi, *Angew. Chem. Int. Ed.*, 2008, **120**, 7840-7844.
35. a) S. Mohani and D. Bonifazi, *Coord. Chem. Rev.*, 2010, **254**, 2342-2362. b) J. Otsuki, *Coord. Chem. Rev.*, 2010, **254**, 2311-2341.
36. L. Grill, M. Dyer, L. Lafferentz, M. Persson, M.V. Peters and S. Hecht, *Nat. Nano.* 2007, **2**, 687-691.
37. a) S.B. Lei, C. Wang, S.X. Yin, H.N. Wang, F. Xi, H.W. Liu, B. Xu, L.J. Wan and C.L. Bai, *J. Phys. Chem. B*, 2001, **105**, 10838-10841. b) J. Otsuki, E. Nagamine, T. Kondo, K. Iwasaki, M. Asakawa and K. Miyake, *J. Am. Chem. Soc.* 2005, **127**, 10400-10405. c) S. Yoshimoto, N. Yokoo, T. Fukuda, N. Kobayashi and K. Itaya, *Chem. Commun.*, 2006, 500 – 502.
38. I. Radivojevic, I. Likhtina, X. Shi, S. Singh and C.M. Drain, *Chem. Commun.*, 2010, **46**, 1643-1645.
39. M. Frieden, M. Giraud, C.B. Reese and Q. Song, *J. Chem. Soc. Perkin Trans. 1*, 1998, 2827 – 2832.
40. M.F. Jacobsen, M.M. Knudsen and K.V. Gothelf, *J. Org. Chem.* 2006, **71**, 9183-9190.
41. (a) C.-H. Lee, F. Li, K. Iwamoto, J. Dadok, A.A. Bothner-By and J.S. Lindsey, *Tetrahedron* 1995, **51**, 11645-11672. (b) P. D. Rao, S. Dhanalekshmi, B. J. Littler and J. S. Lindsey, *J. Org. Chem.* 2000, **65**, 7323-7344. (c) P. D. Rao, B. J. Littler, G. R. Geier III and J.S. Lindsey, *J. Org. Chem.* 2000, **65**, 1084-1092.
42. Y. Choi, C. George, M.J. Comin, J.J. Barchi Jr., H.S. Kim, K.A. Jacobson, J. Balzarini, H. Mitsuya, P.L. Boyer, S.H. Hughes and V.E. Marquez, *J. Med. Chem.* 2003, **46**, 3292-3299.
43. M.C. Etter, *Acc. Chem. Res.*, 1990, **23**, 120-126.
44. (a) R. Taylor, O. Kennard, W. Versichel, *J. Am. Chem. Soc.*, 1983, **105**, 5761-5766. (b) R. Taylor, O. Kennard and W. Versichel, *Acta Cryst.*, 1984, **B40**, 280-288. (c) J. Hamblin, S.P. Argent, A.J. Blake, C. Wilson and N.R. Champness, *CrystEngComm*, 2008, **10**, 1782-1789.
45. (a) A. P. Bisson, C. A. Hunter, J. C. Morales and K. Young, *Chem. Eur. J.*, 1998, **4**, 845-851. (b) A. P. Bisson, F. J. Carver, D. S. Eggleston, R. C. Haltiwanger, C. A. Hunter, D. L. Livingstone, J. F. McCabe, C. Rotger and A. E. Rowan, *J. Am. Chem. Soc.* 2000, **122**, 8856-8868.
46. K. Hoogsteen, *Acta Cryst.*, 1963, **16**, 907-916.
47. J.D. Watson and F.H.C. Crick, *Nature*, 1953, **171**, 737-738.
48. Y. Wei, K. Kannappan, G.W. Flynn and M.B. Zimmt, *J. Am. Chem. Soc.*, 2004, **126**, 5318 – 5322.
49. J.A.A.W. Elemans, I. De Cat, H. Xu and S. De Feyter, *Chem. Soc. Rev.*, 2009, **38**, 722-736.
50. I. Katsumi, H. Kondo, K. Yamashita, T. Hidaka, K. Hosoe, T. Yamashita and K. Watanabe, *Chem. Pharm. Bull.*, 1986, **34**, 121-129
51. S. G. Newman and M. Lautens, *J. Am. Chem. Soc.*, 2010, **132**, 11416-11417.
52. M. A. Fazio, A. Durandin, N. V. Tkachenko, M. Niemi, H. Lemmetyinen and D. I. Schuster, *Chem. Eur. J.*, 2009, **15**, 7698-7705.
53. L. Zhang, J. Fan, K. Vu, K. Hong, J.-Y. Le Brazidec, J. Shi, M. Biamonte, D.J. Busch, R.E. Lough, R. Grecko, Y. Ran, J.L. Sensintaffar, A. Kamal, K. Lundgren, F.J. Burrows, R. Mansfield, G.A. Timony, E.H. Ulm, S.R. Kasibhatla and M.F. Boehm, *J. Med. Chem.*, 2006, **49**, 5352-5362.

## Table of Contents Graphic

